Int. J. Electrochem. Sci., 15 **(2020)** 5487 – 5499, doi: 10.20964/2020.06.22

International Journal of
ELECTROCHEMICAL
SCIENCE
www.electrochemsci.org

Corrosion Inhibition of Carbon Steel in Hydrochloric Acid by *Chrysanthemum Indicum* Extract

Haibing Zhang[1], *Zihui Ni*[2], *Haitao Wu*[1], *Peng Xu*[2], *Zidong Li*[1], *Wuyang Zhang*[1], *Huixian Huang*[1], *Qing Zhou*[1], *Xingui Yue*[1], *Jiankang Bao*[1], *Xueming Li*[2,*]

[1] State Grid Chongqing Electric Power Company, Chongqing 400015, China
[2] School of Chemistry and Chemical Engineering, Chongqing University, Chongqing 400044, China
[*]E–mail: xml301@cqu.edu.cn
[†] Haibing Zhang and Zihui Ni contributed equally to this work.

Received: 6 January 2020 / *Accepted:* 20 February 2020 / *Published:* 10 May 2020

Biodegradable and inexpensive plant extracts are one of the most promising materials for future metal pickling inhibitors. The corrosion inhibition performance of the *Chrysanthemum indicum* extract on carbon steel in 1 mol/L hydrochloric acid solution was evaluated by potentiodynamic polarization, EIS and SEM. Then, FTIR was applied for characterization of functional groups in the *Chrysanthemum indicum* extract. Electrochemical measurement results showed that the inhibition performance of 500 mg/L extract on carbon steel at 25 ^{o}C was up to 93%. The FTIR spectra showed that the extract contained O–H, N–H, C–H, C=C, C–N and C–O groups, which may be the characteristic group of excellent corrosion inhibitor. The adsorption of this inhibitor on the surface of carbon steel is Langmuir adsorption. This study provides an experimental supplement for the applied of plant extracts as metal pickling corrosion inhibitors.

Keywords: corrosion inhibitor, extract, carbon steel, electrochemical test

1. INTRODUCTION

Carbon steel is widely used in the construction of transmission towers due to its excellent mechanical properties and low cost. Generally, the oxidation layer on the surface of the carbon steel needs to be removed by pickling before the carbon steel is processed into transmission tower. Corrosion inhibitors are usually used to inhibit the corrosion of carbon steel during this pickling process. However, the traditional corrosion inhibitors are expensive, difficult to degrade and harmful to the environment and human beings. Therefore, a great deal of efforts have been made in developing low cost, high efficiency and environmentally friendly corrosion inhibitors.

The plant extraction may become corrosion inhibitors due to the advantages of wide sources and biodegradation. It was previously reported that the extracts of *Soybean* [1], *Chenopodium* [2], *Solanum lasiocarpum* [3], *Persian Liquorice* [4], *Ginkgo* [5], *Dacryodis edulis* [6], *Tagetes erecta* [7], *Glycyrrhiza glabra* [8], *Corchorus olitorius* [9], *Saraca ashoka* [10], *Geissospermum* [11], *Cuscuta reflexa* [12], *Ircinia strobilina* [13], *Primula vulgaris* [14], *Tobacco* [15], *Henna* [16], *Asparagus racemosus* [17], *Centaurea cyanus* [18], *Ginger* [19], *Bambusa Arundinacea* [20], *Thymus vulgaris* [21], *Azadirachta indica* [22, 23], *Longan* [24], *Justicia gendarussa* [25], *Salvia officinalis* [26, 27], and *Ficus tikoua* [28] showed excellent corrosion inhibition for carbon steel in acidic medium. Heteroatoms such as nitrogen (N), oxygen (O), sulfur (S) and phosphorus (P) can be used as adsorption centers of inhibitor molecules, and these atoms also have become important features of efficient corrosion inhibitors. The *Chrysanthemum indicum* extract contains 1,8-cineole, camphor, borneol and bornyl acetate, which contain N, O and other heteroatoms [29-32]. Therefore, *Chrysanthemum indicum* extract has the potential to be used as an inhibitor.

In this study, a powdery extract was successfully obtained from *Chrysanthemum indicum* by hot water extraction and subsequent freeze–drying process. The inhibition performance and mechanism of the extract on carbon steel in hydrochloric acid were systematically evaluated by potentiodynamic polarization, electrochemical impedance spectroscopy (EIS), scanning electron microscopy (SEM) and Fourier transformed infrared spectroscopy (FTIR). In addition, the adsorption behavior of extractive inhibitor molecules on the surface of carbon steel was analyzed in detail. This work provides an important reference for plant extracts as corrosion inhibitors for carbon steel pickling.

2. EXPERIMENTAL DETAILS

2.1 Materials

The chemical composition (wt.%) of carbon steel employed for electrochemical experiments and surface analysis are 0.140% C, 0.550% Mn, 0.190% Si, 0.028% P, 0.020% S, and the rest is Fe. Specifically, carbon steel specimens with exposed surfaces of 1.0 cm × 1.0 cm and 0.5 cm × 0.5 cm × 0.5 cm were used for electrochemical experiments and surface analysis, respectively.

For the preparation of the *Chrysanthemum indicum* extract, the procedure was employed according to our previously reported. The dried *Chrysanthemum indicum* was immersed in deionized water at 90 °C for 1 h, and then filtered and concentrated to dryness. Finally, the obtained brown–black viscous substance was freeze–dried for 24 h and crushed into powder.

To evaluate the corrosion inhibition performance of the *Chrysanthemum indicum* extract in acidic environment, the acidic solution used in this study was 1.0 mol/L HCl. All reagents used in this work were of analytical grade and were not purified before use.

2.2 Electrochemical experiments

The inhibition performance of the *Chrysanthemum indicum* extract was systematically evaluated by methods of potentiodynamic polarization and electrochemical impedance spectroscopy (EIS). The electrode was stabilized in 1.0 mol/L HCl solution for 20 min before all electrochemical experiments to achieve steady state. The EIS were measured in the range of 100 kHz – 0.01 Hz with an amplitude of 10 mV. The EIS parameters of carbon steel were obtained by fitting with Zsimpwin software. The range of the potentiodynamic polarization were –300 mV to +300 mV with a scanning rate of 1 mV/s.

2.3 Characterization

The corrosion morphology of carbon steel immersed in 1.0 mol/L HCl solution without and with the *Chrysanthemum indicum* extract was characterized by scanning electron microscopy. FTIR technique over the range from 4000 to 400 cm^{-1} was employed to investigate the groups in the extract.

3. RESULTS AND DISCUSSION

3.1 EIS measurements

The corrosion inhibition performance of the *Chrysanthemum indicum* extract was preliminarily evaluated by EIS measurement. It is worth noting that the OCP–T test was performed for 20 min before all EIS measurements to make the carbon steel electrode reach steady state. As shown in Fig. 1, the Nyquist plots exhibit semicircle in the high frequency region.

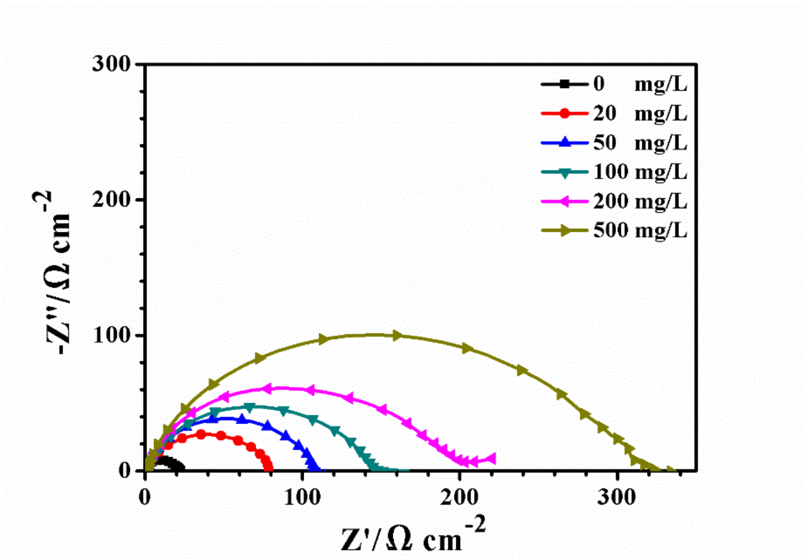

Figure 1. Nyquist diagrams of the carbon steel electrode in hydrochloric acid solutions with 0, 20, 50, 100, 200 and 500 mg/L *Chrysanthemum indicum* extract

Generally, this semicircle in the high frequency region corresponds to the charge transfer resistance (R_{ct}) and the double–layer capacitance (C_{dl}). It is because of the rough surface of the sample or the adsorption of the inhibitor molecules that Nyquist plot appears incomplete semicircle, which is often referred as the frequency dispersion effect. Besides, the diameter of the semicircle in Fig. 1 increases with the increase of the concentration of the corrosion inhibitor, but its shape does not change significantly. Therefore, we conclude that inhibitor molecules form an adsorption film on the surface of carbon steel to suppress the corrosion of carbon steel. However, this adsorption film does not change the corrosion mechanism of carbon steel in hydrochloric acid solution, and the entire corrosion process is still controlled by the charge transfer process. Finally, the diameter of the semicircle reached the maximum with the inhibitor content was 500 mg/L, indicating that the best inhibitor performance was achieved at 500 mg/L.

The impedance data of carbon steel in hydrochloric acid solution was fitted by Zsimpwin software. The equivalent circuit is shown in Fig. 2. The obtained electrochemical parameters are listed in Table 1. Here, Rs is the solution resistance, R_{ct} is the charge transfer resistance, *CPE* is the constant phase angle element, and *CPE* represents the double–layer capacitance (C_{dl}). The definition of *CPE* is as follows:

$$Z_{CPE}=\frac{1}{Y_0(j\omega)^n} \quad (1)$$

where Y_0 is the modulus of the *CPE*, w is the angular frequency, j is the imaginary number ($j^2 = -1$), and n is the dispersion effect index, which reflects the heterogeneity of the electrode surface. When n = 0, *CPE* means resistance, n = –1, it is inductance, and n = 1, it is capacitance.

The value of C_{dl} can be calculated by the following equation :

$$C_{dl}=\frac{Y_0\omega^{n-1}}{\sin(n\pi/2)} \quad (2)$$

The corrosion inhibition performance can be calculated by R_{ct} [33, 34]:

$$\eta_E(\%)=\frac{R_{ct}-R_{ct}^0}{R_{ct}}\times 100 \quad (3)$$

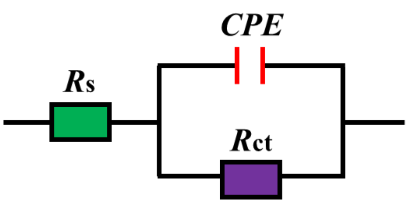

Figure 2. The corresponding equivalent circuits used to fit the experimental EIS data

Table 1 shows that the value of the charge transfer resistance R_{ct} increases as the concentration of the corrosion inhibitor increases, and higher concentrations of the corrosion inhibitor exhibit better corrosion inhibition performance. The corrosion inhibition performance can reach 93% at the inhibitor concentration of 500 mg/L. Compared with the commercial corrosion inhibitor, it has the same level of inhibition performance. In addition, the value of C_{dl} showed a decreasing trend with the increase of the inhibitor concentration, indicating that the adsorption behavior of the inhibitor molecules on the carbon steel surface occurred.

Table 1. EIS fitting parameters with the 0, 20, 50, 100, 200 and 500 mg/L *Chrysanthemum indicum* extract

C (mg/L)	R_s (Ω cm^2)	R_{ct} (Ω cm^2)	Y_0 ($\mu\Omega^{-1}$ s^n cm^{-2})	n	C_{dl} (μF cm^{-2})	η (%)	f (Hz)
0	0.6992	21.02	251.7	0.94	175.78	–	68.1
20	0.7739	76.90	269.9	0.83	125.5	72.7	17.8
50	0.7193	105.9	211.4	0.88	125.05	80.2	14.7
100	0.7730	143.4	263.8	0.81	123.04	85.3	11.2
200	0.7466	193.0	243.4	0.80	120.78	89.1	6.81
500	0.862	300.4	151.2	0.82	80.10	93.0	6.81

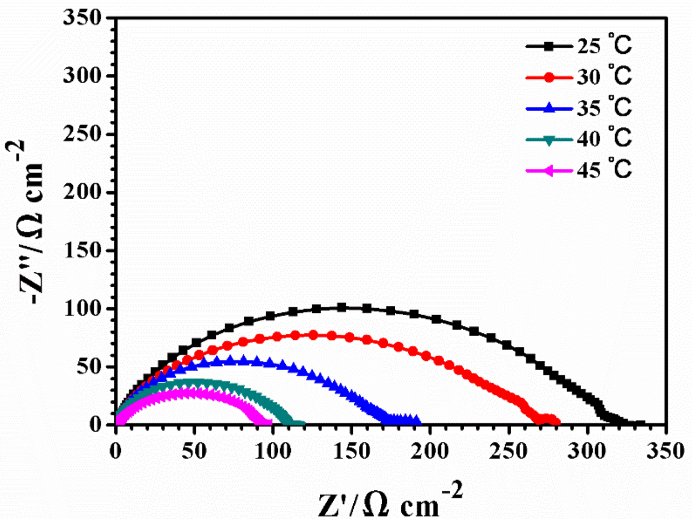

Figure 3. Nyquist diagrams of the carbon steel electrode in hydrochloric acid solutions with 500 mg/L *Chrysanthemum indicum* extract at 25, 30, 35, 40 and 45 °C

Table 2. EIS fitting parameters with the *Chrysanthemum indicum* extract concentrations at 25, 30, 35, 40 and 45 °C.

T (K)	R_s (Ω cm^2)	R_{ct} (Ω cm^2)	Y_0 ($\mu\Omega^{-1}$ s^n cm^{-2})	n	C_{dl} (μF cm^{-2})	η (%)	f (Hz)
25	0.862	300.4	151.2	0.82	80.10	93.0	6.81
30	0.8051	250.3	163.8	0.81	80.97	91.6	8.25
35	0.906	164.6	132.8	0.88	82.30	87.2	10.0
40	0.8176	106.9	217.9	0.84	109.08	80.3	14.7
45	0.94	89.89	344.6	0.76	125.10	76.6	14.7

Furthermore, the effect of temperature on the inhibition performance of the inhibitor is explored in this work. The Nyquist diagram of the *Chrysanthemum indicum* extract in hydrochloric acid solution at 25, 30, 35, 40 and 45 °C is shown in Fig. 3. Obviously, the diameter of Nyquist diagram decreased significantly with the increase of temperature of hydrochloric acid solution. In addition, EIS fitting parameters for the *Chrysanthemum indicum* extract at 25, 30, 35, 40 and 45 ^{o}C are shown in Table 2. The inhibition performance of corrosion inhibitor on carbon steel gradually decreased from 93% at 25 ^{o}C to 76.6% at 45 ^{o}C. In Fig. 4, it can be clearly seen that this corrosion inhibition efficiency changes gradually with temperature.

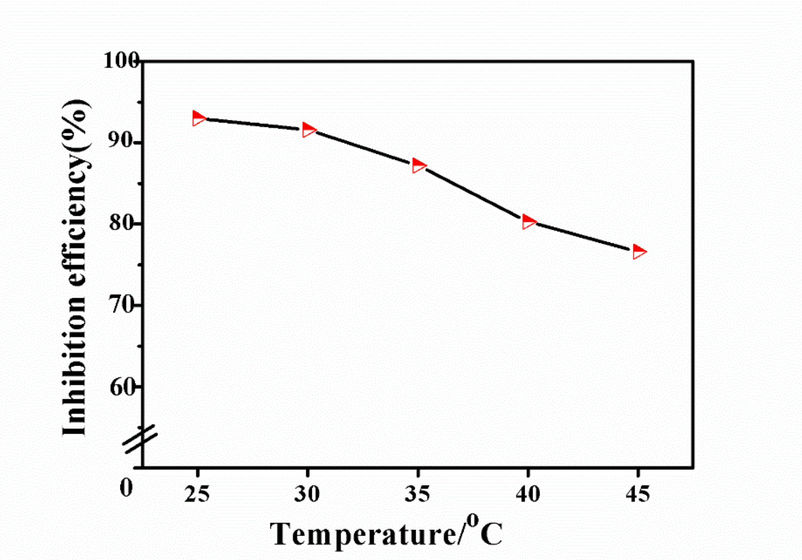

Figure 4. Inhibition efficiency of 500 mg/L *Chrysanthemum indicum* extract on carbon steel in 1 mol/L HCl at different temperatures

In recent years, there are many studies to evaluate the inhibition performance of plant extract inhibitors in acidic solution. The comparison inhibition efficiency of different plant extract inhibitors are shown in Table 3. As can be seen from Table 3, Ficus tikoua extract with concentration of 200 mg/L exhibited excellent corrosion inhibition performance of up to 95.8% for carbon steel in 1 M HCl. Furthermore, ginger extract with 200 ppm concentration also showed 94% inhibition performance on carbon steel in 1 M HCl. In contrast, *Chrysanthemum Indicum* extract prepared in this work showed better corrosion inhibition performance for carbon steel in HCl acid. Specifically, the inhibition performance of 500 mg/L *Chrysanthemum Indicum* extract on carbon steel at 25 ^{o}C was up to 93%. The inhibition performances of plant extract inhibitors are different because of different preparation methods of plant extracts.

Table 3. Comparison of inhibition efficiency for different plant extract inhibitors

Inhibition	Concentration	Acid medium	Inhibition efficiency (%)	Reference
Dacryodis edulis	800 mg/L	1 M HCl	66.0	[6]
Primula vulgaris	1000 ppm	1 M HCl	95.5	[14]
Henna	300 ppm	1 M HCl	83.1	[16]
Ginger	200 ppm	1 M HCl	94.0	[19]
Ficus tikoua	200 mg/L	1 M HCl	95.8	[28]
Chrysanthemum Indicum	500 mg/L	1 M HCl	93.0	This work

3.2 Potentiodynamic polarization measurements

The potentiodynamic polarization curves of carbon steel electrode in hydrochloric acid solution with the 0, 20, 50, 100, 200 and 500 mg/L corrosion inhibitor are shown in Fig. 5. It can be seen that the cathode part of the polarization curve moves towards the direction of low current density after the corrosion inhibitor is added. Moreover, with the increase of corrosion inhibitor concentration, the greater the movement range is, indicating that corrosion inhibitor has a significant inhibitory performance on the cathode reaction of carbon steel in hydrochloric acid solution. In addition, the anode part of the polarization curve was close to coincidence with the blank solution or increased, indicating that the corrosion inhibitor had no inhibitory performance on the anodic reaction of carbon steel in hydrochloric acid solution.

The corrosion inhibition performance of the extract can be calculated by extrapolating the i_{corr} from the potentiodynamic polarization curves [35, 36]:

$$\eta_p(\%)=\frac{i^0_{corr}-i_{corr}}{i^0_{corr}}\times 100 \qquad (4)$$

Electrochemical parameters (E_{corr}, i_{corr}, β_a, β_c, η) were obtained through the extrapolation method shown in Table 4. It can be seen from Table 4 that, the current density gradually decreases with the increasing concentration of the inhibitor, indicating that the addition of the inhibitor can slow down the corrosion of carbon steel in hydrochloric acid. All E_{corr} displacements were less than 85 mV compared to the blank solution, suggesting that the plant extract could be treated as mixed–type inhibitor. The maximum inhibition efficiency of this plant extract on carbon steel in 1 mol/L hydrochloric acid can reach 88.57% from the potentiodynamic polarization measurements. The corrosion inhibition properties obtained by potentiodynamic polarization curves and EIS are in good agreement.

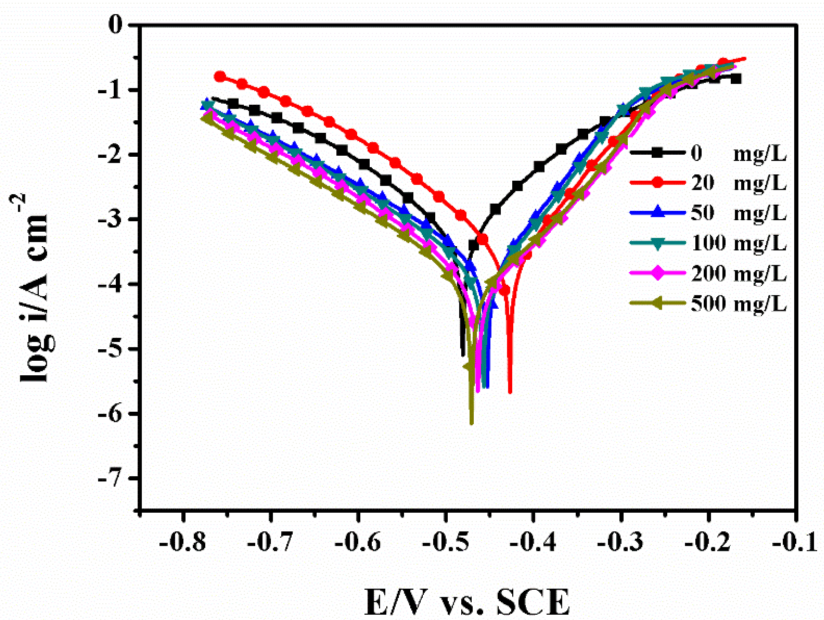

Figure 5. Polarization curves of the carbon steel electrode in hydrochloric acid solutions with the 0, 20, 50, 100, 200 and 500 mg/L *Chrysanthemum indicum* extract

Table 4. Polarization parameters derived from Tafel plots of carbon steel immersed in 1 mol/L HCl containing the *Chrysanthemum indicum* extract at different concentrations

C (mg/L)	E_{corr} (mV vs. SCE)	i_{corr} (μA cm^{-2})
0	–481	597.4
20	–427	232.8
50	−453	180.6
100	–457	132.7
200	–464	68.46
500	−471	68.26

The corrosion inhibition performances of 500 mg/L inhibitor at 25, 30, 35, 40 and 45 °C were further investigated. As shown in Fig. 6, the polarization curve gradually moves towards the direction of high current with the increase of temperature. This phenomenon means that the effect of the inhibitor decays as the temperature rises. Table 5 exhibits the polarization parameters of carbon steel soaks with 1 mol/L HCl containing 500 mg/L inhibitor at different temperatures. It can be clearly seen from Table 5 that the inhibition performance of the inhibitor will decline significantly with the increase of temperature, reaching 49.65% at 45 °C. These results indicate that the corrosion inhibition performance of the extract is not well at high temperature. This is really a serious problem, which will limit the practical application of the *Chrysanthemum indicum* extract. The strategy to improve the corrosion inhibition performance of plant extracts at high temperature should be further explored in future research.

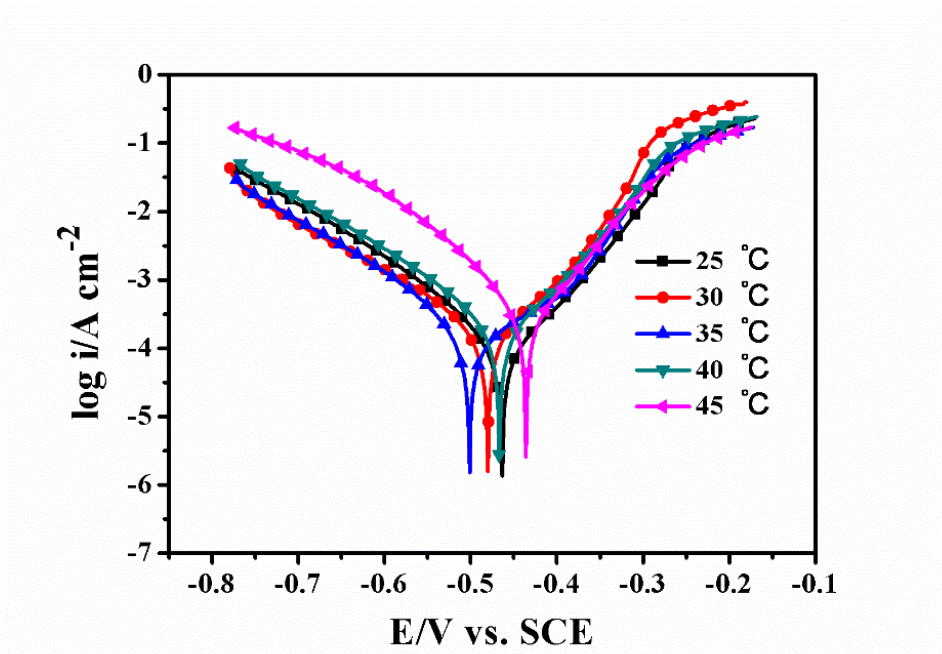

Figure 6. Polarization curves of the *Chrysanthemum indicum* extract in hydrochloric acid solutions at 25, 30, 35, 40 and 45 °C

Table 5. Polarization parameters derived from Tafel plots of carbon steel immersed in 1 mol/L HCl containing the *Chrysanthemum indicum* extract at different temperatures

T (K)	E_{corr} (mV vs. SCE)	i_{corr} (μA cm^{-2})
25	−471	68.26
30	–480	114.3
35	–501	125.4
40	–467	162.3
45	–463	300.8

3.3 Adsorption isotherm

To further understand the adsorption mechanism of the *Chrysanthemum indicum* extract, the adsorption isotherm was drawn by the following equation [37-41]:

$$\frac{C_{inh}}{\theta} = \frac{1}{K_{ads}} + C_{inh} \qquad (5)$$

where C_{inh} is the concentration of the *Chrysanthemum indicum* extract, θ stand for the surface coverage (defined as θ), and K_{ads} is the adsorption equilibrium constant. As shown in Fig. 7, the fitting line has a high linear regression coefficient ($R^2 = 0.9994$), which means that the adsorption mechanism of the *Chrysanthemum indicum* extract can be described by Langmuir isothermal adsorption.

It is worth noting here that the molecular mass of the *Chrysanthemum indicum* extract is uncertain. Therefore, we cannot calculate the adsorption energy of this inhibitor to further determine whether the adsorption mechanism is physical adsorption or chemical adsorption.

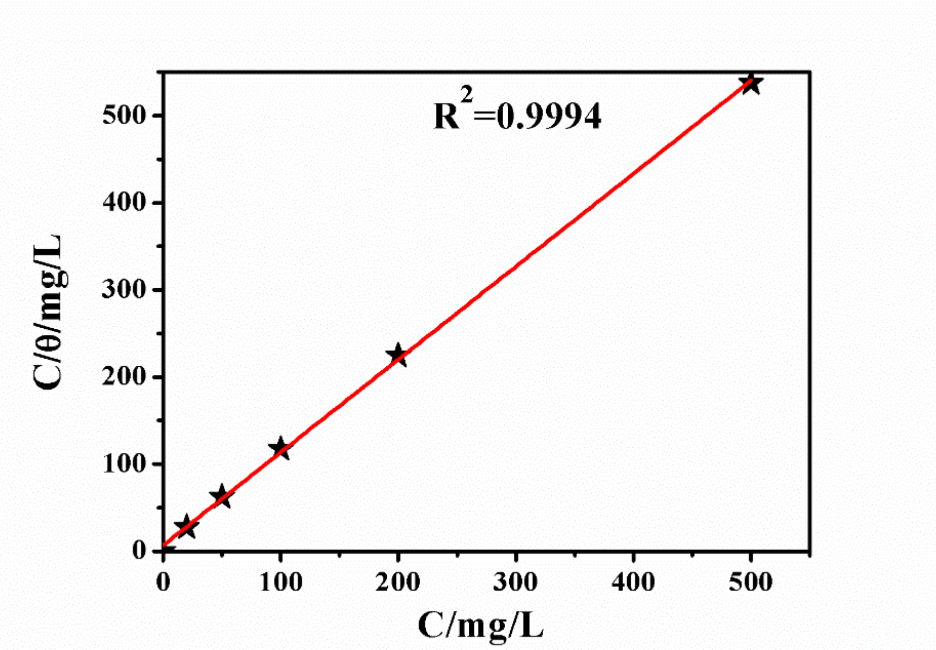

Figure 7. Langmuir adsorption isotherms of the *Chrysanthemum indicum* extract for carbon steel in 1 mol/L HCl solution at 298 K

3.4 FTIR

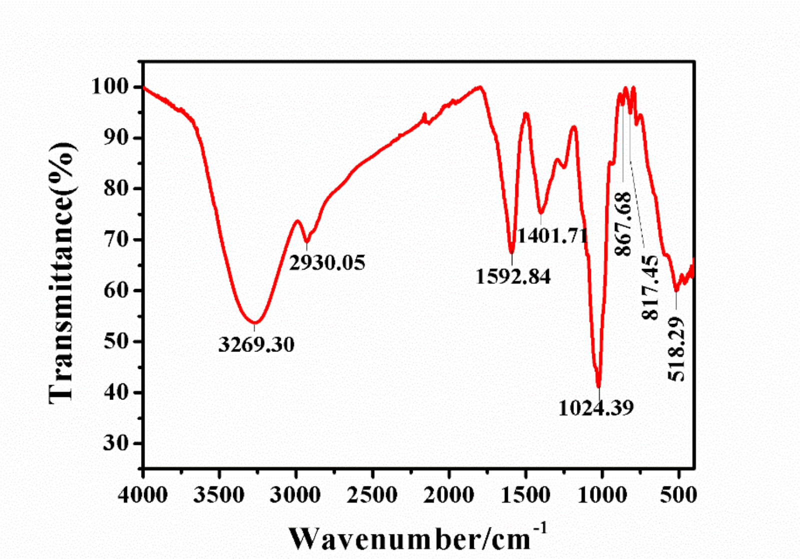

Figure 8. FTIR spectra of the *Chrysanthemum indicum* extract

The FTIR analysis was performed to characterize the functional groups involved in the *Chrysanthemum indicum* extract. Fig. 8 shows FTIR spectra of the *Chrysanthemum indicum* extract. The adsorption band at 3269 cm^{-1} assigned to O–H or N–H group, peaks at 2930.5, 1401.71, 867.68, 817.45 and 518.29 cm^{-1} attributed to C–H group, a peak at 1592.84 cm^{-1} due to the presence of C=C group and a peak at 1024.39 cm^{-1} corresponding to C–N or C–O group [42-44]. These results indicate that there are O–H, N–H, C–H, C=C, C–N and C–O groups in the *Chrysanthemum indicum* extract, which can reveal the inhibition mechanism of this inhibitor.

3.5 Surface characterization

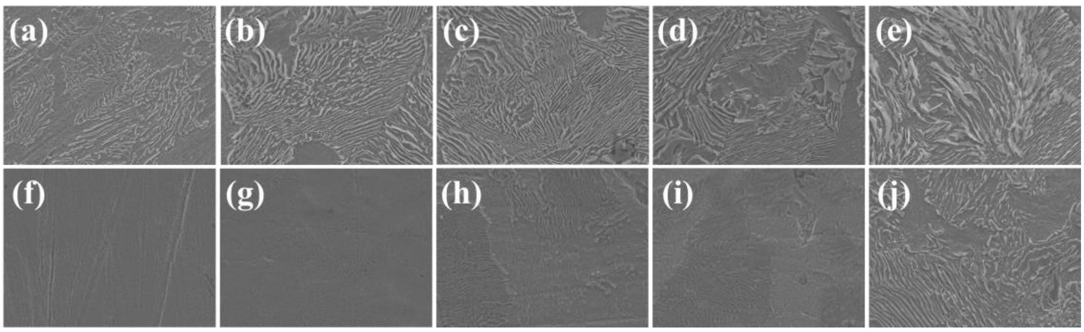

Figure 9. SEM images of carbon steel without 500 mg/L inhibitor at (a) 25 °C, (b) 30 °C, (c) 35 °C, (d) 40 °C, and (e) 45 °C after immersion in 1 mol/L HCl for 20 min; with 500 mg/L inhibitor at (f) 25 °C, (g) 30 °C, (h) 35 °C, (i) 40 °C and (j) 45 °C after immersion in 1 mol/L HCl for 20 min

The SEM was used to characterize the corrosion morphology of carbon steel electrodes after electrochemical measurements. Fig. 9 (a–e) exhibits the corrosion morphology of the carbon steel electrode etched for 30 min in hydrochloric acid solution with a concentration of 500 mg/L of the extract inhibitor at 25–45 ^oC, respectively. Besides, Fig. 9 (f–j) also shows the corrosion morphology of carbon steel electrode etched for 30 min in blank hydrochloric acid solution at 25–45 ^oC, respectively. It can be seen from Fig. 8 that inhibitors have a great impact on the corrosion behavior of carbon steel. Corrosion behavior of carbon steel in hydrochloric acid solution can be significantly inhibited by the inhibitors at the same temperature. In Fig. 8 (a–b), we can even observe the scratches left by sandpaper on the surface of the carbon steel. However, a large number of corrosion pits have been formed on the surface of the carbon steel in Fig. 9 (f–g). These results proved the excellent corrosion inhibition performance of *Chrysanthemum indicum* extracts on carbon steel in hydrochloric acid.

Moreover, corrosion inhibition performance of corrosion inhibitor on carbon steel gradually decreases with the increase of temperature. As shown in Fig. 8 (a–e), the corrosion of carbon steel is gradually intensified and the corrosion pits are gradually aggravated with the increase of temperature. This result is consistent with the results of the previous electrochemical measurements.

4. CONCLUSION

In this work, the *Chrysanthemum indicum* extract was obtained by hot water extraction and subsequent freeze–drying process. The corrosion inhibition performance of *Chrysanthemum indicum* extract on carbon steel in hydrochloric acid was investigated by electrochemical measurements. Moreover, the main functional groups in the *Chrysanthemum indicum* extract was characterized by FTIR. The results show that the *Chrysanthemum indicum* extract shows excellent corrosion inhibition performance for carbon steel in hydrochloric acid, and belongs to mixed–type inhibitor inhibitor. The adsorption of this inhibitor on the surface of carbon steel is Langmuir adsorption. The corrosion inhibitor forms a dense adsorption layer on the surface of carbon steel, which plays a role in inhibiting the corrosion of carbon steel in hydrochloric acid.

ACKNOWLEDGEMENTS
This work was supported by Chongqing Graduate Research and Innovation Project (No. CXB14220), Chongqing Municipal Training Program of Innovation and Entrepreneurship for Undergraduates (No. S201910611427) and National Natural Science Foundation of China (No. 61271059).

References

1. A.M. El-Azaly, *Int. J. Electrochem. Sci*., 14 (2019) 2714-2731.
2. M. M. Motawea, *Int. J. Electrochem. Sci*., 14 (2019) 1372-1387.
3. X. Wang, *Int. J. Electrochem. Sci.*, 14 (2019) 1178-1196.
4. E. Alibakhshi, M. Ramezanzadeh, S.A. Haddadi, G. Bahlakeh, B. Ramezanzadeh, M. Mandavian, *J. Cleaner Prod.*, 210 (2019) 660-672.
5. S. Deng, X. Li, *Corros. Sci.*, 55 (2012) 407-415.
6. E.E. Oguzie, C.K. Enenebeaku, C.O. Akalezi, S.C. Okoro, A.A. Ayuk, E.N. Ejike, *J. Colloid*

Interface Sci., 349 (2010) 283-292.
7. P. Mourya, S. Banerjee, M.M. Singh, *Corros. Sci*., 85 (2014) 352-363.
8. E. Alibakhshi, M. Ramezanzadeh, G. Bahlakeh, B. Ramezanzadeh, M. Mahdavian, M. Motamedi, *J. Mol. Liq.*, 255 (2018) 185-198.
9. M. Gobara, B. Zaghloul, A. Baraka, M. Elsayed, M. Zorainy, M.M. Kotb, H. Elnabarawy, *Mater. Res. Express*, 4 (2017) 046504.
10. A. Saxena, D. Prasad, R. Haldhar, G. Singh, A. Kumar, *J. Mol. Liq*., 258 (2018) 89-97.
11. M. Faustin, A. Maciuk, P. Salvin, C. Roos, M. Lebrini, *Corros. Sci*., 92 (2015) 287-300.
12. A. Saxena, D. Prasad, R. Haldhar, *Bioelectrochemistry*, 124 (2018) 156-164.
13. C.M. Fernandes, T.d.S. Ferreira Fagundes, N.E. dos Santos, T.S.d.M. Rocha, R. Garrett, R.M. Borges, G. Muricy, A.L. Valverde, E.A. Ponzio, *Electrochim. Acta*, 312 (2019) 137-148.
14. M.T. Majd, S. Asaldoust, G. Bahlakeh, B. Ramezanzadeh, M. Ramezanzadeh, *J. Mol. Liq*., 284 (2019) 658-674.
15. Y. Guo, M. Gao, H. Wang, Z. Liu, *Int. J. Electrochem. Sci*., 12 (2017) 1401-1420.
16. A.S. Fouda, M.M. Hegazi, A. El-Azaly, *Int. J. Electrochem. Sci*., 14 (2019) 4668-4682.
17. A. Saxena, D. Prasad, R. Haldhar, *J. Mater. Sci.*, 53 (2018) 8523-8535.
18. F.E.T. Heakal, M.A. Deyab, M.M. Osman, A.E. Elkholy, *Desalination*, 425 (2018) 111-122.
19. H.S. Gadow, M.M. Motawea, *Rsc Adv.*, 7 (2017) 24576-24588.
20. S.A. Asipita, M. Ismail, M.Z. Abd Majid, Z.A. Majid, C. Abdullah, J. Mirza, *J. Cleaner Prod.*, 67 (2014) 139-146.
21. A. Ehsani, M.G. Mahjani, M. Hosseini, R. Safari, R. Moshrefi, H. Mohammad Shiri, *J. Colloid Interface Sci*., 490 (2017) 444-451.
22. B.S. Swaroop, S.N. Victoria, R. Manivannan, *J. Taiwan Inst. Chem. Eng*., 64 (2016) 269-278.
23. L. Valek, S. Martinez, *Mater. Lett*., 61 (2007) 148-151.
24. L.L. Liao, S. Mo, H.Q. Luo, N.B. Li, *J. Colloid Interface Sci*., 499 (2017) 110-119.
25. A.K. Satapathy, G. Gunasekaran, S.C. Sahoo, K. Amit, P.V. Rodrigues, *Corros. Sci*., 51 (2009) 2848-2856.
26. Y. Lekbach, Z. Li, D. Xu, S. El Abed, Y. Dong, D. Liu, T. Gu, S.I. Koraichi, K. Yang, F. Wang, Bioelectrochemistry (Amsterdam, Netherlands), 128 (2019) 193-203.
27. N. Soltani, N. Tavakkoli, M. Khayatkashani, M.R. Jalali, A. Mosavizade, *Corros. Sci*., 62 (2012) 122-135.
28. Q. Wang, B. Tan, H. Bao, Y. Xie, Y. Mou, P. Li, D. Chen, Y. Shi, X. Li, W. Yang, *Bioelectrochemistry*, 128 (2019) 49-55.
29. Z. Shunying, Y. Yang, Y. Huaidong, Y. Yue, Z. Guolin, *J. Ethnopharmacol*., 96 (2005) 151-158.
30. C. Kim, M.C. Kim, S.M. Kim, D. Nam, S.H. Choi, S.H. Kim, K.S. Ahn, E.H. Lee, S.H. Jung, K.S. Ahn, *Phytother. Res*., 27 (2013) 30-38.
31. G.B. Shi, M.H. Zhao, Q.C. Zhao, Y. Huang, Y.F. Chen, *Phytomedicine*, 18 (2011) 609-616.
32. C. Zhang, M.J. Qin, P. Shu, J.L. Hong, L. Lue, D.X. He, *Chem. Biodiversity*, 7 (2010) 2951-2962.
33. X. Guo, C. Lai, X. Jiang, W. Mi, Y. Yin, X. Li, Y. Shu, *Chem. Eng. J.*, 335 (2018) 843-854.
34. X.L. Jiang, C. Lai, Z. Xiang, J. Tang, L. Liu, Y.T. Gu, R.S. Wu, Z.R. Wu, J.J. Yuan, D.Q. Hou, Y.C. Zhang, *Int. J. Electrochem. Sci*., 13 (2018) 6462-6472.
35. C. Lai, J. Cao, Y.F. Deng, Y.F. Yang, X. Wen, Z.L. Wang, C.W. Fan, Y.N. Shi, Y. Li, J.L. Li, C.L. Yang, Y.J. Yang, W. Pang, Y. Liu, *Int. J. Electrochem. Sci*., 14 (2019) 10259-10269.
36. C. Lai, B. Xie, X. Guo, Phosphorus Sulfur Relat. Elem., 195 (2020) 107-114.
37. L. Feng, *Int. J. Electrochem. Sci*., 12 (2017) 1915-1928.
38. B. Tan, S. Zhang, H. Liu, Y. Guo, Y. Qiang, W. Li, L. Guo, C. Xu, S. Chen, *J. Colloid Interface Sci*., 538 (2019) 519-529.
39. Y. Qiang, S. Zhang, B. Tan, S. Chen, *Corros. Sci*., 133 (2018) 6-16.
40. B. Tan, S. Zhang, Y. Qiang, L. Feng, C. Liao, Y. Xu, S. Chen, *J. Mol. Liq*., 248 (2017) 902-910.
41. B. Tan, S. Zhang, Y. Qiang, W. Li, H. Li, L. Feng, L. Guo, C. Xu, S. Chen, G. Zhang, *J. Mol. Liq*.,

298 (2017) 111975.
42. C. Wang, J. Chen, B. Hu, Z. Liu, C. Wang, J. Han, M. Su, Y. Li, C. Li, *J. Cleaner Prod.*, 238 (2019) 117823.
43. H. Derfouf, Y. Harek, L. Larabi, W. J. Basirun, M. Ladan, *J. Adhes. Sci. Technol.*, 33 (2019) 808-833.
44. NZN. Hashima, EH. Anouarb, K. Kassimc, HM. Zakic, AI. Alharthib, Z. Embonge, *Appl. Surf. Sci.*, 476 (2019) 861-877.